



NMR Time Reversal as a Probe of Incipient Turbulent Spin Dynamics

M. E. Hayden,¹ E. Baudin,² G. Tastevin,² and P. J. Nacher²

¹*Physics Department, Simon Fraser University, 8888 University Drive, Burnaby BC, Canada V5A 1S6*

²*Laboratoire Kastler Brossel, Ecole Normale Supérieure; CNRS; UPMC; 24 rue Lhomond, F75005 Paris, France*

(Received 23 April 2007; published 27 September 2007)

We demonstrate time reversal of nuclear spin dynamics in highly magnetized dilute liquid ^3He - ^4He mixtures through effective inversion of long-range dipolar interactions. These experiments, which involve using magic sandwich NMR pulse sequences to generate spin echoes, probe the spatiotemporal development of turbulent spin dynamics and promise to serve as a versatile tool for the study and control of dynamic magnetization instabilities. We also show that a repeated magic sandwich pulse sequence can be used to dynamically stabilize modes of nuclear precession that are otherwise intrinsically unstable. To date, we have extended the effective precession lifetimes of our magnetized samples by more than three orders of magnitude.

DOI: [10.1103/PhysRevLett.99.137602](https://doi.org/10.1103/PhysRevLett.99.137602)

PACS numbers: 82.56.Jn, 75.50.Mm, 76.60.Jx, 76.60.Lz

Elementary treatments of nuclear magnetic resonance (NMR) ignore collective effects. Individual spin dynamics are assumed to be independent of the sample magnetization \mathbf{M} , and are thus governed by linear differential equations. This approximation is justified for many—but certainly not all—practical applications. One of the most well known and pervasive counter examples is the phenomenon of radiation damping [1], in which the emf induced in the pickup coil by \mathbf{M} drives a current; the magnetic field associated with this current in turn acts on \mathbf{M} , driving it into alignment with the static field \mathbf{B}_0 in a nonlinear manner. A less common but more insidious problem arises when the magnetic field produced by the magnetized sample becomes large enough to directly influence spin dynamics [2–6]. This leads to a rich variety of nonlinear effects that range from spectral clustering to precession instabilities and spin turbulence. The former arises when small-angle NMR tipping pulses are applied to the sample (generating small angular displacements of \mathbf{M} from \mathbf{B}_0), and is manifest by the spontaneous appearance of long-lived geometry-dependent modes of coherent nuclear precession. The latter occurs when large-angle tipping pulses are employed, and involves an exponential growth in the complexity of spatially inhomogeneous magnetization patterns. Far from being mere curiosities, phenomena arising from nonlocal interactions (including the joint action of “distant dipolar fields” and radiation damping [7,8]) threaten to limit (or profoundly alter) the operation of state-of-the-art high-field high-resolution NMR spectrometers. They are equally important for understanding the dynamics of polarized quantum fluids including Bose-Einstein condensates [9], superfluid ^3He [10,11], degenerate ^3He - ^4He mixtures [12], and two-dimensional H gases [13]. From yet another perspective, the collective effects induced by distant dipolar fields can be used to amplify weak spin precession signals [14] and to enhance the sensitivity of precision searches for CP -violating permanent electric dipole moments [5].

Here we describe NMR time reversal experiments that—for the first time—shed light on the extent to which the deleterious effects of spin turbulence can be controlled or suppressed. Moreover, they lay the foundation for a systematic and quantitative investigation of the onset of dynamical magnetization instabilities under diverse conditions. Our experiments are performed on dilute non-degenerate mixtures of hyperpolarized ^3He in liquid ^4He . They are based on the use of magic sandwich (MS) pulse sequences [15,16]: continuous bursts of tipping pulses that are appropriately timed and phased so as to refocus spin dynamics associated with dipolar interactions, leading to the formation of echoes. The MS pulse cycle and numerous variants are indispensable tools in the field of solid-state NMR but, to the best of our knowledge, have not been used previously for liquid-state NMR [17].

Our samples are confined to a slightly-prolate 0.44 cm^3 spheroidal Pyrex cell treated with Cs metal to suppress wall relaxation [18,19], and are maintained at temperatures $T \sim 1\text{ K}$. The sample cell communicates with a room temperature metastability-exchange optical pumping cell and various gas reservoirs via a narrow Pyrex tube. The entire apparatus is immersed in a 2.3 mT magnetic field shimmed to $\pm 20\text{ ppm}$ over the sample cell and actively stabilized to $\pm 10\text{ ppm}$ against fluctuations in the background laboratory field. We control the volume of liquid admitted to the cell (typically 40% full), the concentration X of ^3He in the mixture (typically 1–5%), and the nuclear polarization (typically $\lesssim 40\%$). We can thus manipulate the shape of the sample, the initial amplitude of its magnetization M , and the ^3He diffusion coefficient D . Note that it is convenient to report M in terms of a characteristic dipolar field $B_{\text{dip}} = \mu_0 M$ or dipolar frequency $F_{\text{dip}} = \gamma B_{\text{dip}}/2\pi$, where μ_0 is the permeability of free space and γ is the ^3He gyromagnetic ratio.

Our pulsed NMR experiments are performed at 74 kHz using orthogonal transmit and receive coils. The transmit coils are actively-shielded [20] to suppress the induction of

eddy currents in nearby conducting structures. This enables us to apply the intense and sustained rf (i.e., \mathbf{B}_1) fields that are necessary for NMR time reversal experiments without causing the sample to warm. It also ensures that eddy currents do not distort the applied rf field, which is uniform to within ± 200 ppm over the sample cell. The receive coils are tuned in a tank configuration with a quality factor $Q_0 \sim 10$. The filling factor η is of order 0.02 when the cell is completely full, and an externally adjustable “ Q -spoiling” resistor is used to ensure that radiation damping fields are small compared to those generated by the magnetized sample. Typically, a value $Q \sim 2$ was employed for the work presented here.

Figure 1 summarizes data from two experiments that illustrate some of the unusual behavior exhibited by highly magnetized liquids. The first experiment involves application of a single 90° rf tipping pulse. The corresponding free induction decay (FID) is shown as trace (a). The signal amplitude S is roughly constant for several tens of ms, during which time the precessing transverse nuclear magnetization is necessarily uniform. This is followed by a precipitous drop that culminates in a number of small revivals. Similar experiments performed over a range of initial conditions indicate that the characteristic time scale for the abrupt decrease in signal amplitude (i.e., $T_{1/2}$) is inversely proportional to B_{dip} [21].

Evidence that this behavior is not dominated by terms in the equation of motion linear in \mathbf{M} is provided by the

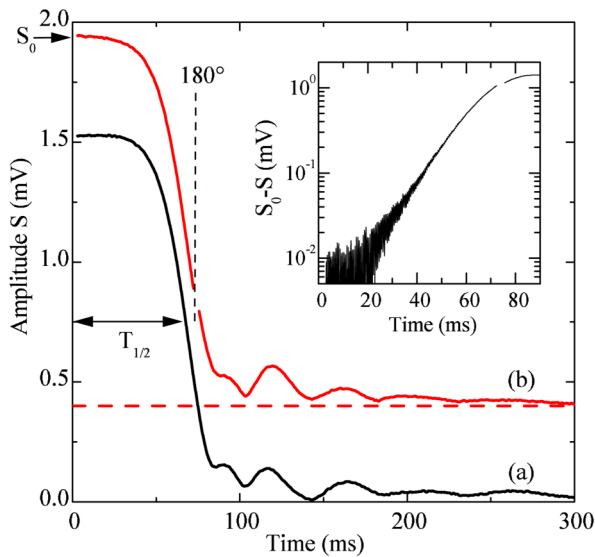


FIG. 1 (color online). FID response of polarized ^3He in liquid ^4He (a) to a 90° rf tipping pulse and (b) to a 90° - τ - 180° sequence. The time at which the FID amplitude S drops to half of its initial value S_0 is denoted $T_{1/2}$, which is of order 70 ms for these examples. Trace (b) has been displaced upward by 0.4 mV for the sake of clarity. The inset shows the deviation of trace (b) from its initial amplitude. These data were acquired at $T = 1.14$ K, with $X \sim 2\%$ and $B_{\text{dip}} \sim 0.9$ μT for trace (a) and $X \sim 5\%$ and $B_{\text{dip}} = 0.7$ μT for trace (b).

second experiment, in which the initial 90° pulse is followed 70 ms later by a 180° pulse. Comparison of traces (a) and (b) reveals that the 180° pulse has little if any effect on the FID envelope. In particular, there is no obvious sign of a Hahn (or inhomogeneous) spin echo 140 ms after the start of the experiment. Closer examination of these data shows that the deviation of the FID amplitude S from its initial value S_0 grows exponentially with time t (inset to Fig. 1): i.e., $S_0 - S \sim \exp(2\Gamma t)$. This behavior is expected for an infinite spin system dominated by distant dipolar interactions [6], and has been interpreted as the onset of spin turbulence [3]. We have performed exact numerical simulations of these experiments for small numbers of dipolar-coupled spins diffusing on a cubic lattice (up to $32 \times 32 \times 32$ sites) with periodic boundary conditions [21], and observe excellent agreement between measured and calculated growth rates. In both cases $\Gamma/F_{\text{dip}} \sim 2.3$, which is somewhat smaller than the value $2\sqrt{2}\pi/3 \sim 3.0$ predicted for an infinite spin system [6].

The experimental challenge presented by these data is to devise a method for probing the spatial and temporal evolution of the nuclear magnetization before, during, and *after* the point at which it spontaneously and abruptly averages to zero in Fig. 1. The approach we explore here as a first step toward this goal is the application of MS pulse sequences to reverse the effective time evolution of dynamics associated with dipolar interactions, and thereby attempt to generate spin echoes. Thorough descriptions of the manner in which time reversal is accomplished can be found in the literature [15]. For our purposes the essential features of these multiple-pulse sequences are that (a) the applied rf field must be large compared to the dipolar fields and (b) the effective rate at which the dipolar-coupled system evolves in time as the rf fields are applied is scaled by a factor of $-1/2$.

Figure 2 shows data from several experiments that are analogous to the ineffective 90° - τ - 180° sequence of Fig. 1 except for the fact that the 180° tipping pulse has been replaced with MS sequences of various durations. The rf used for these sequences is typically adjusted to be within 1 Hz of the ^3He Larmor frequency. The most striking and important feature of these data is that large NMR signals are detected long after the net transverse magnetization normally would have averaged to zero. The upper half of Fig. 2 shows data from three experiments that progressively “unwind” the state of the dipolar-coupled system back to times $t = 2\tau/3$, $t = \tau/3$, and $t = 0$, as indicated by the paired-symbols \blacksquare , \bullet , \blacktriangle . The initial amplitudes of these echoes nominally probe the amplitude of the “rotary echo” [15,22] that is formed in the doubly-rotating frame [23] during the MS sequence. In the first case—trace (a)—the magnitude of the transverse magnetization is returned to a value that is close to that which is anticipated. Moreover, the shape of the ensuing FID mimics the original decay (cf. Figure 1). In the last case—trace (c)—the amplitude of the signal following the MS starts out notice-

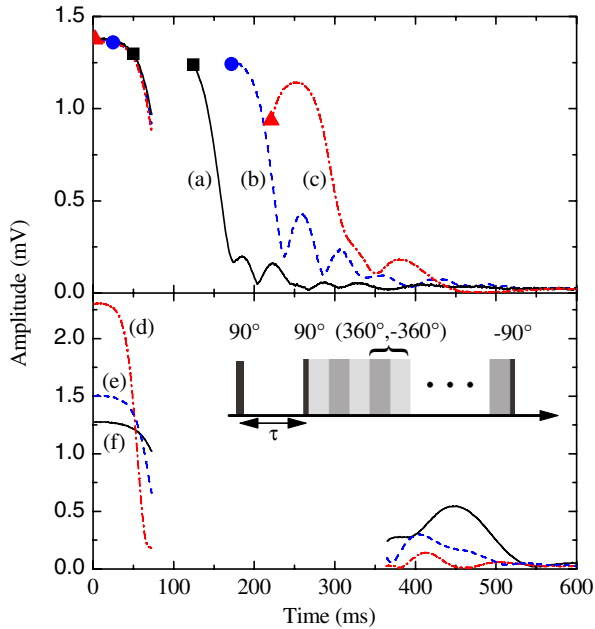


FIG. 2 (color online). Spin echo formation: A 90° pulse is applied at $t = 0$, after which the magnetization is allowed to evolve for $\tau = 70$ ms. MS sequences of various durations are then used to progressively refocus the magnetization. For traces (a)–(c), the amplitude of the FID immediately after the MS probes the rotary echo formed in the doubly-rotating frame. The symbols \blacksquare , \bullet , \blacktriangle indicate pairings between points on the initial FID to which the state of the magnetization is nominally returned and the ensuing free precession signal. For traces (d)–(f), the amplitude of the FID probes the magic sandwich echo formed in the rotating frame after the magnetization is first “unwound” back to $t = -\tau$ before being “released” and allowed to undergo further free evolution. These data were acquired under conditions similar to those outlined in Fig. 1. Inset: A classic magic sandwich [15] consists of a continuous train of $(180_x^\circ, -180_x^\circ)$ rotation pairs sandwiched between a leading 90_y° and a trailing -90_y° rotation. We have used 360° (rather than 180°) rotations to reduce the accumulation of phase errors associated with offsets between the rf and Larmor frequencies. Each 360° rotation is accomplished in 2 ms, corresponding to $B_1 = 15 \mu\text{T}$. Note that for trace (c), the sense of the terminal 90° rotation was reversed (i.e., 90_y° instead of -90_y°) in order to also refocus interactions with a linear dependence on \mathbf{M} . This does not significantly alter the initial amplitude of the echo or its subsequent growth.

ably smaller than anticipated but then unexpectedly grows rather than decaying. Clearly, the deficit in the initial echo amplitude is not associated with an irreversible process. The shape of the FID labeled (b) is qualitatively intermediate between traces (a) and (c). The lower part of Fig. 2 shows data from three experiments that nominally “unwind” the state of the dipolar-coupled system back to a time $t = -\tau$, resulting in the formation of a “magic sandwich echo” in the rotating frame [15] after a further free evolution period of duration τ . Increasing the initial magnetization increases the rate at which magnetization pat-

terns develop, and so this series of experiments effectively probes the sample at successively later stages of evolution.

It is not surprising that we observe imperfect refocusing of the transverse nuclear magnetization in these experiments. Irreversible processes (e.g., diffusion) necessarily compete with the spatiotemporal evolution of the magnetization and progressively attenuate structures on larger and larger scales as time progresses. At the same time, while the MS tends to refocus the family of magnetization patterns that develop during the initial FID, one expects a complementary family of instabilities [6] to be established and grow during the time reversal sequence. Technical imperfections in the time reversal sequence will also contribute to echo attenuation. A detailed and systematic study of these rich and complex effects is required before quantitative statements can be made regarding the onset and development of spin turbulence.

The fact that spin echoes *can* be generated in highly magnetized liquids leads one to contemplate the use of more sophisticated NMR tools. To illustrate this point, we describe here a simple but significant extension of the basic MS sequence that clearly merits further investigation. A conventional CPMG sequence ($90^\circ - \tau - 180^\circ - 2\tau - 180^\circ - 2\tau \dots$) acts on a system dominated by interactions that are linear in \mathbf{M} , repeatedly inverting the phase of the precessing magnetization to produce an echo train. By analogy, a Repeated Magic Sandwich (RMS) sequence consisting of a train of MS cycles interspersed with appropriate delays should likewise act on a system dominated by distant dipolar interactions to form an echo train. The validity of this conjecture is borne out by the data shown in Fig. 3. The RMS sequence used to generate these data is of the form ($90^\circ - \tau - \text{MS} - 2\tau - \text{MS} - 2\tau \dots$), where the duration of each MS cycle is 4τ (i.e., long enough to effectively “reverse” the time evolution of the dipolar-coupled system for a time 2τ). The four traces correspond to experiments performed with different delay times τ . In each case, the RMS sequence is applied for ~ 9 s, at which point \mathbf{M} is allowed to evolve without further interruption.

Figure 3 reveals two distinct phases in the evolution of the magnetization during the application of RMS sequences. Each echo train starts with a period that we associate with imperfect refocusing of the magnetization. That is, behavior similar to the examples presented in Fig. 2. Increasing the length of time during which the magnetization is allowed to evolve between successive magic sandwiches results in greater losses. This initial period is followed by a second phase during which magnetization losses continue to be incurred, but at significantly lower rates. Comparison with Figs. 1 and 2 reveals that the apparent lifetimes of these dynamically sustained precession signals are in some cases more than 3 orders of magnitude longer than the characteristic coherence time (e.g., $T_{1/2}$) of the freely evolving magnetization. Exact numerical simulations of these experiments (analogous to

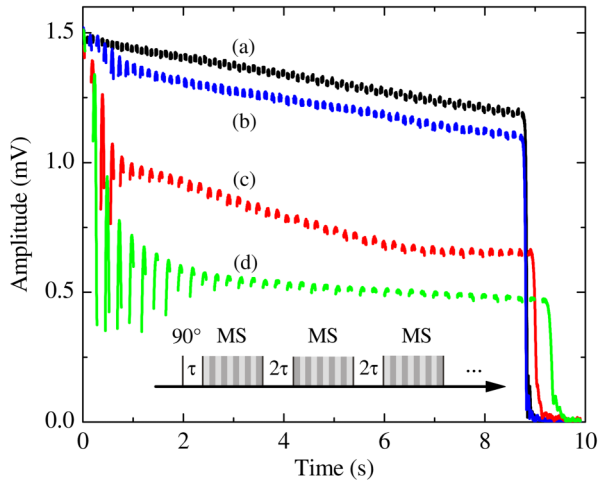


FIG. 3 (color online). Spin echo trains: Traces (a)–(d) correspond to echo trains that are observed when RMS sequences with delay times $\tau = 16, 24, 32,$ and 40 ms, respectively, are applied to the magnetized liquid. The MS cycles used to obtain these data are identical to those described in the caption of Fig. 2 except for the facts that each one terminates with an additional 180_y° rotation (cf. trace (c) of Fig. 2) to refocus interactions linear in \mathbf{M} , and that the symmetry of alternate MS cycles is inverted to reduce the accumulation of phase errors. That is, odd MS cycles are of the form $[90_y^\circ, n \times (360_x^\circ, -360_x^\circ), 90_y^\circ]$ while even MS cycles are of the form $[-90_y^\circ, n \times (-360_x^\circ, 360_x^\circ), -90_y^\circ]$. These data were acquired at $T \sim 1.1$ K, with $X \sim 4.5\%$ and $B_{\text{dip}} \sim 0.8 \mu\text{T}$. In the limit $B_{\text{dip}} \rightarrow 0$, CPMG-based measurements yield $D \sim 2 \times 10^{-7} \text{ m}^2/\text{s}$.

those described above) have been used to investigate the influence of diffusion and rf field amplitude. They reveal similar—but not identical—behavior. The initial period during which losses are incurred is observed, as is the transition to a second evolutionary phase and the dependence of this transition on both τ and B_{dip} . On the other hand, our model calculations yield a steady state solution for which we are not able to resolve a decay rate: that is, a plateau. This suggests that our experimentally-determined echo trains may yet be limited by systematic rather than intrinsic effects. One possibility is the small but finite heat load placed on our cryostat by eddy currents induced during RMS sequences, which would in turn lead to evaporation of ^3He atoms. Another possibility is imperfect refocusing of the magnetization caused by imperfect phasing of rf tipping pulses. Finally, it is worth commenting on the terminal FID at the end of each RMS sequence. Analysis of these decays yields values of Γ that are proportional to the terminal echo amplitude and consistent with those observed following a single 90° tipping pulse (cf. Figure 1). This strongly suggests that the precessing magnetization is highly uniform at the peak of each revival, and that the “seeds” from which instabilities ultimately develop [6] are small.

In summary, we have demonstrated the production of NMR spin echoes and spin echo trains in magnetized

liquids under conditions where nuclear spin dynamics (in the rotating frame) are dominated by nonlinear and non-local (or distant) dipolar interactions. Our experiments, which are based on the use of magic sandwich time reversal pulse sequences, probe the rich spatiotemporal evolution of the nuclear magnetization distribution that results from competition between nonlinear spin dynamics and diffusion. They promise to yield quantitative information about the progression and extent of disorder, as well as new methods to control or suppress the onset of instabilities.

M. H. gratefully acknowledges support from the CNRS (France), the ENS (Paris), and NSERC (Canada).

- [1] e.g. A. Vlassenbroek, J. Jeener, and P. Broekaert, *J. Chem. Phys.* **103**, 5886 (1995), and references therein.
- [2] D. Candela, M. E. Hayden, and P. J. Nacher, *Phys. Rev. Lett.* **73**, 2587 (1994).
- [3] J. Jeener, *Phys. Rev. Lett.* **82**, 1772 (1999).
- [4] K. L. Sauer *et al.*, *Phys. Rev. B* **63**, 184427 (2001).
- [5] M. P. Ledbetter and M. V. Romalis, *Phys. Rev. Lett.* **89**, 287601 (2002).
- [6] J. Jeener, *J. Chem. Phys.* **116**, 8439 (2002).
- [7] Y. Y. Lin *et al.*, *Science* **290**, 118 (2000).
- [8] e.g. S. Datta, S. Y. Huang, and Y. Y. Lin, *Concepts Magn. Reson.* **28A**, 410 (2006), and references therein.
- [9] S. Giovanazzi, A. Görlitz, and T. Pfau, *Phys. Rev. Lett.* **89**, 130401 (2002).
- [10] A. S. Borovik-Romanov *et al.*, *JETP Lett.* **40**, 1033 (1984).
- [11] L. R. Corruccini and D. D. Osheroff, *Phys. Rev. B* **17**, 126 (1978).
- [12] e.g. S. Perisanu and G. Vermeulen, *Phys. Rev. B* **73**, 214519 (2006) and references therein.
- [13] S. Vasilyev *et al.*, *Phys. Rev. Lett.* **89**, 153002 (2002).
- [14] M. P. Ledbetter, I. M. Savukov, and M. V. Romalis, *Phys. Rev. Lett.* **94**, 060801 (2005).
- [15] W.-K. Rhim, A. Pines, and J. S. Waugh, *Phys. Rev. B* **3**, 684 (1971).
- [16] e.g. S. Hafner, D. E. Demco, and R. Kimmich, *Solid State Nucl. Magn. Reson.* **6**, 275 (1996), and references therein.
- [17] In solid-state NMR, one is usually concerned with strong anisotropic interactions between small numbers of neighboring spins. In liquid-state NMR, molecular motions average these local interactions to zero. The distant dipolar fields encountered in our experiments arise from the combined effect of *all* spins in the highly magnetized sample.
- [18] Wall contributions to the NMR relaxation times T_1 and T_2 are of order several hours under these conditions.
- [19] N. Piegay and G. Tastevin, *J. Low Temp. Phys.* **126**, 157 (2002).
- [20] C. P. Bidinosti, I. S. Kravchuk, and M. E. Hayden, *J. Magn. Reson.* **177**, 31 (2005).
- [21] P. J. Nacher *et al.*, *J. Low Temp. Phys.* **126**, 145 (2002).
- [22] H. Kessemeier and W. K. Rhim, *Phys. Rev. B* **5**, 761 (1972).
- [23] A. G. Redfield, *Phys. Rev.* **98**, 1787 (1955).